

THREE-DIMENSIONAL VIBRATORY CHARACTERISTICS OF SOLID CYLINDERS AND SOME REMARKS ON SIMPLIFIED BEAM THEORIES

K. M. LIEW and K. C. HUNG

Division of Engineering Mechanics, School of Mechanical and Production Engineering,
Nanyang Technological University, Singapore 2263

(Received 7 July 1994; in revised form 1 December 1994)

Abstract—A set of linear three-dimensional frequency equations that describes the vibratory characteristics of elastic solid cylinders of different end supports is derived. Starting from the linear, small-strain, three-dimensional elasticity theory, integral expressions for strain and kinetic energies are formulated. The three-dimensional mode shapes are expressed in terms of sets of one- and two-dimensional orthogonal polynomial functions which are to approximate the longitudinal and lateral surface variations of solid cylinders. From the resulting displacement-based energy expressions, the variational form of the three-dimensional energy functional is minimized to yield the linear eigenvalue equation. Frequency solutions for elastic solid cylinders of different lengths and end support conditions are determined. The accuracy of solutions is validated through convergence tests and comparisons with the existing three-dimensional analytical solutions and empirical data. From the present three-dimensional elasticity solutions, some remarks on the existing simplified beam theories are made. Particular attention is drawn to Timoshenko's shear deformable beam theory for transverse bending modes. The validity of the one-dimensional wave equation for longitudinal and torsional modes is also discussed.

1. INTRODUCTION

In this paper, the governing frequency equation of elastic solid cylinders with various combinations of end support conditions is derived. Developed on the basis of the linear, small-strain, three-dimensional elasticity theory in conjunction with an extremum energy principle, the method is capable of extracting all possible modes of vibration for elastic solid cylinders. Insofar as the natural modes of cylinders is concerned, there exist three distinct families of vibration motions: (1) longitudinal extensional modes, (2) axial torsional modes and (3) transverse bending modes. Furthermore, coupling among the axial torsional and transverse bending modes also occurred for some special cases. The vibratory characteristic of solid cylinders can be approximated from the existing simplified analytical models. These models give reasonably accurate predictions with minimum numerical arithmetic. The one-dimensional wave equation, in particular, has been commonly applied to obtain frequency solutions for axial torsional and extensional wave motions. These results have been well documented in several text books dealing with the subject of structural dynamics (Timoshenko *et al.* 1974; Harker, 1983).

Within the context of classical theory, the Bernoulli–Euler beam equation has been widely acclaimed for its simplicity and accuracy in providing solutions to transverse vibrations of slender beams and columns. This theory, however, is found to be inadequate for cases in which the beam dimensions cannot be regarded as slender, for example, deep beams or higher vibratory modes. Therefore, various refined beam theories have been proposed to provide a better simulation of beam dynamic characterisation. Notable development in this direction is attributed to Timoshenko (1921, 1922). The complicating effects due to shear deformation and rotary inertia have been considered. Frequency results computed on the basis of Timoshenko's theory abound in the literature. Extensive research on the choice of the correction factors to account for non-uniform shear stress distribution over the cross section has also been reported (Cowper, 1966; Spence and Seldin, 1970; Stephen, 1978).

It is important, when applying these simplified models, to know the underlying assumptions and limitations of the theories to the vibration analysis of beams and cylinders. Research has been conducted to establish the bounds governing the use of these simplified theories to solve engineering problems. Hutchinson (1980, 1981), for instance, used a series type solution technique with Bessel functions as its basis to obtain the symmetric and unsymmetric vibration results for a stress free cylinder of finite length. Based on the three-dimensional elasticity solutions, he has commented in depth on the validity and range of applicability of Timoshenko's beam theory.

Apart from the works of Hutchinson (1980, 1981), further three-dimensional frequency results for elastic solid cylinders of different end support conditions have also been documented by other researchers using different approaches (Armenakes *et al.*, 1969; McMahon, 1970; Gladwell and Tabbildar, 1972; Gladwell and Vijay, 1975; Visscher *et al.*, 1991; Heyliger and Jilani, 1992). In view of the practical importance of these structures in contemporary industrial practice, the present work is carried out firstly, to supplement the existing frequency data for circular cylinders with various combinations of end support conditions, and secondly, to compare, based on the present three-dimensional elasticity solutions, the discrepancies of the classical and refined theories in predicting the proper vibration of three-dimensional solid cylinders. For this purpose, the governing frequency equation is derived from the three-dimensional linear, small-strain elasticity theory. In the solution process, the integral expressions of strain and kinetic energies are expressed in terms of sets of orthogonally constructed one- and two-dimensional polynomial functions. These functions approximate the longitudinal and lateral surface variations of the elastic solid. To arrive at the eigenvalue matrix, the displacement-based energy functional (consisting of the maximum strain and kinetic energy expressions) is minimized according to the Ritz procedure. Solving iteratively for the zeros of the determinant yields the three-dimensional frequency results. From the symmetry inherent in circular cylinders, the vibration mode shapes are conveniently classified into four distinct symmetry classes: (1) the double-symmetry (SS) mode; (2) the symmetry-antisymmetry (SA) mode; (3) the antisymmetry-symmetry (AS) mode and (4) the double-antisymmetry (AA) mode.

In this paper, the accuracy and reliability of the results obtained are established through extensive convergence study. Comparison with the analytical solutions of Hutchinson (1981) and the benchmarking experimental results of McMahon (1964) is conducted. Sets of first known frequency solutions covering wide ranges of length-to-diameter ratios and different boundary conditions are presented. Three-dimensional vibration mode shapes for selected cases are also included for future reference.

2. METHOD OF SOLUTION

Consider a homogeneous, isotropic, linear elastic solid cylinder of length L and diameter a as shown in Fig. 1. The orientation of the cylinder is defined on a Cartesian coordinate system (x_1, x_2, x_3) located at the end $x_3 = 0$ with its origin coinciding with the centroid of the cross section. For this study, it is assumed that except for the two ends at $x_3 = 0$ and L , the other surfaces are free from stresses. The global displacements at a generic point are resolved into three orthogonal components, u_1 , u_2 (lateral) and u_3 (longitudinal), respectively.

2.1. Elastic strain and kinetic energy expressions

The integral expression of the maximum elastic strain energy, in three-dimensions, is given by

$$V_{\max} = \frac{\Delta}{2} \int_R \int_0^L \left[v \left(\sum_{i=1}^3 U_{i,i} \right)^2 + (1-2v) \left(\sum_{i=1}^3 U_{i,i}^2 \right) + \frac{1}{2} (1-2v) \{ (U_{1,2} + U_{2,1})^2 + (U_{2,3} + U_{3,2})^2 + (U_{1,3} + U_{3,1})^2 \} \right] dx_3 dx_2 dx_1 \quad (1)$$

where

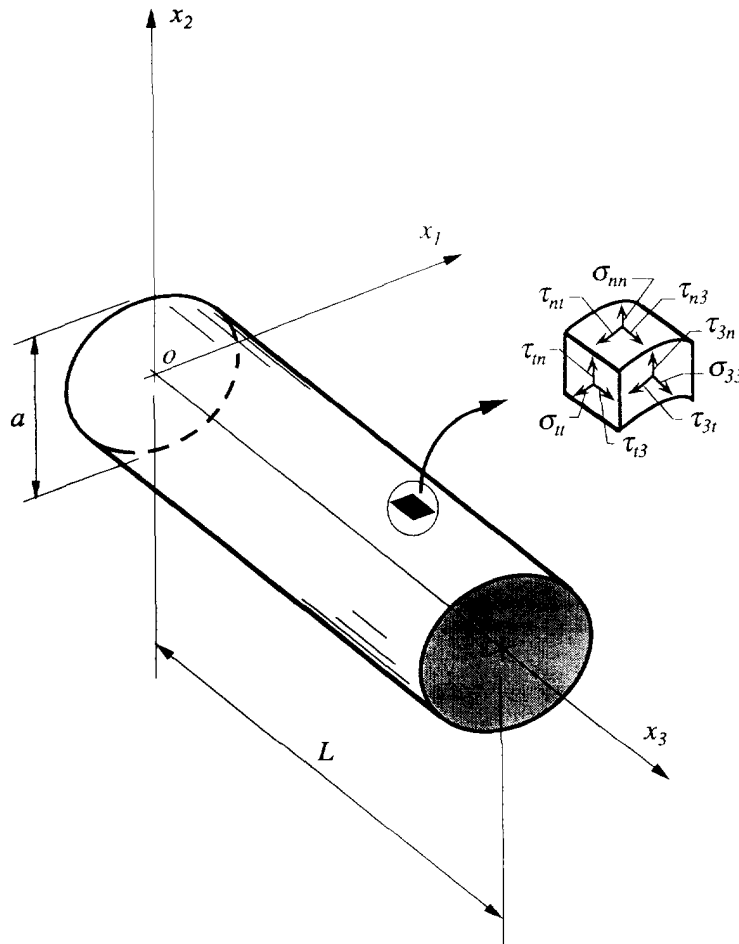


Fig. 1. Geometry and dimensions of an elastic circular cylinder and the notations of stress components.

$$\Delta = \frac{E}{(1 + \nu)(1 - 2\nu)} \tag{2}$$

in which \$E\$ is the Young's modulus and \$\nu\$ the Poisson ratio.

The maximum kinetic energy for free vibration is given by

$$T_{\max} = \frac{\rho\omega^2}{2} \int \int_R \int_0^L \left(\sum_{i=1}^3 U_i^2 \right) dx_3 dx_2 dx_1 \tag{3}$$

where \$\rho\$ is the mass density per unit volume. The double integrals in eqns (1) and (3) are performed over the area \$R\$ of the circular cross section.

2.2 The admissible lateral and longitudinal polynomial functions

The displacement amplitude functions, \$U_i(x_1, x_2, x_3)\$, \$i = 1, 2, 3\$ assume the form of truncated double polynomial series in one- and two-dimensions; expressed as follows,

$$U_i(x_1, x_2, x_3) = \sum_{m=1}^M \sum_{n=1}^N C_{mn}^i \phi_m^i(x_1, x_2) \psi_n^i(x_3); \quad i = 1, 2, 3 \tag{4}$$

in which \$C_{mn}^i\$, \$i = 1, 2, 3\$ are the unknown coefficients to be determined.

Table 1. The two-dimensional basic functions used in each symmetry class of vibration

Symmetry class	Surface function		
	$\phi_1^1(x_1, x_2)$	$\phi_1^2(x_1, x_2)$	$\phi_1^3(x_1, x_2)$
SS	x_1	x_2	1
SA	x_1x_2	1	x_2
AS	1	x_1x_2	x_1
AA	x_2	x_1	x_1x_2

The two-dimensional polynomials, $\phi_m^i(x_1, x_2)$ approximate the lateral surface variations of each displacement component. The one-dimensional polynomials, $\psi_n^i(x_3)$, on the other hand, approximate the displacement variations in the longitudinal direction.

The two-dimensional surface functions are intrinsically sets of admissible functions which are products of a two-dimensional orthogonal polynomial space and a basic function. The detailed method of construction of these polynomials can be found in Liew *et al.* (1994).

The choice of the basic function, $\phi_1^i(x_1, x_2)$, is chosen to satisfy the free wall conditions of the cylindrical elastic solids. The corresponding boundary conditions are

$$\sigma_{nn} = \tau_{nt} = \tau_{n3} = 0 \tag{5}$$

where n and t are the coordinate normal and tangent to the wall boundary; σ_{nn} is the normal stress, τ_{nt} and τ_{n3} are the shear stresses as shown in Fig. 1. Due to the symmetry inherent in the geometry of the cross section, the vibration mode shapes can be conveniently classified into symmetry and antisymmetry modes about the x_1x_3 and x_2x_3 planes. In the computation process, the basic functions assumed for the lateral surface are given in Table 1 for each symmetry mode.

The one-dimensional polynomial function in the longitudinal direction is much easier to generate since it involves only a single variable. These functions are constructed from the Gram-Schmidt recurrence formula which has been demonstrated by Liew *et al.* (1993).

The basic functions, $\psi_1^i(x_3)$, in the longitudinal direction are defined by the products of the respective boundary expression at each end, i.e.

$$\psi_1^i(x_3) = (x_3)^{\Omega_1^i} (x_3 - L)^{\Omega_2^i} \tag{6}$$

where Ω_x^i ($i = 1, 2$ and 3 ; $\alpha = 1, 2$) are the basic powers of the boundary expression. The boundary condition for an end at $x_3 = L$ (corresponding to $\alpha = 2$) is defined as follows:

- stress free condition

$$\sigma_{33} = 0, \quad \tau_{31} = 0 \quad \text{and} \quad \tau_{32} = 0 \tag{7a}$$

- simply supported condition

$$u_1 = 0, \quad u_2 = 0 \quad \text{and} \quad \sigma_{33} = 0 \tag{7b}$$

- fully clamped condition

$$u_1 = 0, \quad u_2 = 0 \quad \text{and} \quad u_3 = 0. \tag{7c}$$

The corresponding value of the basic power is chosen to satisfy the geometric boundary conditions at both ends of the cylinder:

$$\bullet \Omega_x^1 = \begin{cases} 0 & \text{if the } x\text{th end is stress free;} \\ 1 & \text{if the } x\text{th end is simply supported or clamped.} \end{cases} \quad (8a)$$

$$\bullet \Omega_x^2 = \begin{cases} 0 & \text{if the } x\text{th end is stress free;} \\ 1 & \text{if the } x\text{th end is simply supported or clamped.} \end{cases} \quad (8b)$$

$$\bullet \Omega_x^3 = \begin{cases} 0 & \text{if the } x\text{th end is stress free or simply supported;} \\ 1 & \text{if the } x\text{th end is clamped.} \end{cases} \quad (8c)$$

2.3. Linear eigenvalue equation in three-dimensional setting

Let Π be the energy functional given by

$$\Pi = V_{\max} - T_{\max} \quad (9)$$

This functional is minimized according to the Ritz minimum energy principle,

$$\frac{\partial \Pi}{\partial C_{mn}^i} = 0; \quad i = 1, 2, 3 \quad (10)$$

which leads to the governing eigenvalue equation of the form,

$$\left(\begin{bmatrix} \mathbf{k}^{11} & \mathbf{k}^{12} & \mathbf{k}^{13} \\ & \mathbf{k}^{22} & \mathbf{k}^{23} \\ \text{Sym} & & \mathbf{k}^{33} \end{bmatrix} - \lambda^2 \begin{bmatrix} \mathbf{m}^{11} & 0 & 0 \\ & \mathbf{m}^{22} & 0 \\ \text{Sym} & & \mathbf{m}^{33} \end{bmatrix} \right) \begin{Bmatrix} \mathbf{C}^1 \\ \mathbf{C}^2 \\ \mathbf{C}^3 \end{Bmatrix} = \begin{Bmatrix} \mathbf{0} \\ \mathbf{0} \\ \mathbf{0} \end{Bmatrix} \quad (11)$$

where the eigenvalue of the cylinder is given by:

$$\lambda = \omega a \sqrt{\rho/E}. \quad (12)$$

The explicit form of the respective elements in the stiffness and mass submatrices are similar to those reported by Liew *et al.* (1994).

3. NUMERICAL APPLICATIONS

Having derived the governing linear eigenvalue equation for the three-dimensional free vibration of elastic solid cylinders, a standard QR algorithm is utilized to find the roots (i.e. eigenvalues) of the determinant. Frequency parameters, $\lambda = \omega a \sqrt{\rho/E}$, for cylinders of different lengths and end support conditions have been computed. Three-dimensional deformed mode shapes for some selected cases are presented to provide a better insight to the vibratory characteristics of this problem.

In the numerical examples presented, the symbol *F* denotes a free edge, *S* a simply supported edge and *C* a clamped edge. Consequently, the notation *C-F* identifies a cylinder with cantilevered end support condition. The present formulation is catered specifically for isotropic material that follows Hooke’s law of linear elasticity. The Poisson ratio of the material is taken to be $\nu = 0.3$ throughout the present study unless otherwise stated. To establish the results, convergence tests have been conducted. Whenever possible, the converged results are compared with the existing three-dimensional analytical solutions and empirical data from the literature.

3.1 Computational results

The convergence of numerical solutions is demonstrated for a cylinder with length-to-diameter ratio of $L/a = 2.0$. The degree of polynomial, *p*, for surface functions and the number of terms, *q*, for longitudinal functions have been varied in different steps to show the relative effects on the rate of convergence. The frequency solutions, as shown in

Table 2. Convergence of frequency parameters, $\lambda = \omega a \sqrt{\rho/E}$, for an elastic circular cylinder with stress free ends (Diameter = a , $L/a = 2.0$ and $\nu = 0.3$)

Symmetry classes	Orders of polynomials	Mode sequence number					
		1	2	3	4	5	6
SS mode	$p = 5, q = 5$	1.5467	2.6265	2.6612	2.8855	2.9128	3.0209
	$p = 6, q = 5$	1.5467	2.6265	2.6612	2.8855	2.9128	3.0209
	$p = 5, q = 6$	1.5467	2.6265	2.6612	2.8855	2.9128	3.0209
	$p = 5, q = 7$	1.5467	2.6265	2.6612	2.8855	2.9128	3.0209
SA mode	$p = 5, q = 5$	0.9594	1.7751	2.5938	2.6386	3.3820	3.4505
	$p = 6, q = 5$	0.9594	1.7751	2.5938	2.6386	3.3820	3.4505
	$p = 5, q = 6$	0.9594	1.7751	2.5937	2.6386	3.3818	3.4481
	$p = 5, q = 7$	0.9594	1.7751	2.5937	2.6386	3.3818	3.4481
AA mode	$p = 5, q = 5$	0.9742	1.9483	2.6267	2.6615	2.9128	2.9225
	$p = 6, q = 5$	0.9742	1.9483	2.6267	2.6615	2.9128	2.9225
	$p = 5, q = 6$	0.9742	1.9483	2.6267	2.6615	2.9128	2.9225
	$p = 5, q = 7$	0.9742	1.9483	2.6267	2.6615	2.9128	2.9225
	$p = 5, q = 8$	0.9742	1.9483	2.6267	2.6615	2.9128	2.9225

Table 2 for a stress free solid circular cylinder, are found to be invariant to the order of polynomial, p , used in the lateral surface functions. Significant improvement in the convergence, however, is achieved by increasing the number of terms, q , employed in the longitudinal function.

To investigate further the effect of end support conditions on the rate of convergence, cylinders with $C-F$, $S-S$ and $C-C$ end support conditions are examined. Table 3 demonstrates the effect of different end supports on the convergence pattern. It is found that cylinders with higher constraints at the ends need a higher number of terms to attain a reasonable convergence. From the convergence study, it is decided that $p = 5$ and $q = 10$ are to be used for all computations in this study.

3.2 Vibration mode shapes

The vibratory response of solid cylinders can be further clarified by considering the deformed mode shapes at each symmetry class. The three-dimensional deformed mode

Table 3. Convergence of frequency parameters, $\lambda = \omega a \sqrt{\rho/E}$, for an elastic circular cylinder with different ends conditions (Diameter = a , $L/a = 2.0$ and $\nu = 0.3$)

Boundary conditions	Orders of polynomials	Symmetry classes and mode sequence number								
		SS-1	SS-2	SS-3	SA-1	SA-2	SA-3	AA-1	AA-2	AA-3
$C-F$	$p = 5, q = 5$	0.7948	2.3095	2.6458	0.1985	0.8080	1.7283	0.4871	1.4615	2.4618
	$p = 6, q = 5$	0.7948	2.3095	2.6458	0.1985	0.8080	1.7283	0.4871	1.4615	2.4618
	$p = 5, q = 6$	0.7942	2.3077	2.6446	0.1981	0.8071	1.7186	0.4871	1.4613	2.4389
	$p = 5, q = 7$	0.7938	2.3068	2.6444	0.1978	0.8067	1.7160	0.4871	1.4612	2.4357
	$p = 5, q = 8$	0.7936	2.3061	2.6444	0.1977	0.8064	1.7156	0.4871	1.4612	2.4354
	$p = 5, q = 9$	0.7935	2.3057	2.6443	0.1976	0.8062	1.7153	0.4871	1.4612	2.4354
$S-S$	$p = 5, q = 5$	0.7934	2.3055	2.6443	0.1976	0.8061	1.7152	0.4871	1.4612	2.4354
	$p = 5, q = 5$	1.5467	2.8703	2.8856	0.4965	1.4278	2.2838	0.9742	1.9483	2.8705
	$p = 6, q = 5$	1.5467	2.8703	2.8856	0.4965	1.4278	2.2838	0.9742	1.9483	2.8705
	$p = 5, q = 6$	1.5467	2.8703	2.8856	0.4965	1.4278	2.2838	0.9742	1.9483	2.8704
	$p = 5, q = 7$	1.5467	2.8703	2.8856	0.4965	1.4278	2.2838	0.9742	1.9483	2.8703
	$p = 5, q = 8$	1.5467	2.8703	2.8856	0.4965	1.4278	2.2838	0.9742	1.9483	2.8703
$C-C$	$p = 5, q = 9$	1.5467	2.8703	2.8856	0.4965	1.4278	2.2836	0.9742	1.9483	2.8703
	$p = 5, q = 10$	1.5467	2.8703	2.8856	0.4965	1.4278	2.2838	0.9742	1.9483	2.8703
	$p = 5, q = 5$	1.5949	2.9552	3.0271	0.7756	1.5472	2.4749	0.9742	1.9483	2.9225
	$p = 6, q = 5$	1.5949	2.9552	3.0271	0.7756	1.5472	2.4749	0.9744	1.9483	2.9282
	$p = 5, q = 6$	1.5945	2.9552	3.0266	0.7754	1.5470	2.4747	0.9743	1.9483	2.9282
	$p = 5, q = 7$	1.5944	2.9551	3.0263	0.7753	1.5469	2.4746	0.9742	1.9483	2.9226
$C-C$	$p = 5, q = 8$	1.5943	2.9551	3.0262	0.7752	1.5469	2.4745	0.9742	1.9483	2.9226
	$p = 5, q = 9$	1.5942	2.9551	3.0261	0.7752	1.5469	2.4745	0.9742	1.9483	2.9225
	$p = 5, q = 10$	1.5942	2.9551	3.0261	0.7752	1.5469	2.4745	0.9742	1.9483	2.9225
		1.5942	2.9551	3.0261	0.7752	1.5469	2.4745	0.9742	1.9483	2.9225

shapes and corresponding frequency parameters for cylinders of $L/a = 2.0$ with $F-F$, $C-F$, $S-S$ and $C-C$ end support conditions are depicted in Fig. 2. Due to the symmetry inherent in the circular cross section, the deformed mode shapes can be conveniently classified into: (1) double-symmetry (SS), (2) symmetry-antisymmetry (SA), (3) antisymmetry-symmetry (AS) and (4) double-antisymmetry (AA) modes about the x_1x_3 and x_2x_3 planes. It should be noted that the SA and AS modes for the circular cross section share an identical frequency value. The first three modes of vibration at each symmetry class are presented. From Fig. 2, it is observed that the fundamental SS mode is predominantly a longitudinal extensional mode and transverse bending motion is observed at the first and second SA modes. First and second order axial torsional motions are found to occur at AA-1 and AA-2 modes.

In Fig. 2, the influences of end support conditions on the deformed mode shapes are examined. Generally, it is found that the transverse bending motion at SA-1 possesses the lowest vibration frequency parameter. This is followed by the first order torsional motion at AA-1. The longitudinal extensional motion has much higher frequency. It is also noted that the SS-2 and AA-3 modes for circular cylinder with $F-F$ end support condition deformed in a similar manner with an identical frequency parameter ($\lambda = 2.6265$). Comparing the deformed mode shapes at different support conditions, it is further noticed that the first torsional mode of circular cylinders with $F-F$, $S-S$ and $C-C$ boundary conditions has an identical torsional frequency parameter ($\lambda = 0.9742$).

3.3 Comparison of analytical and empirical results

Hutchinson (1980, 1981) used a series type solution technique with displacements assumed in Bessel functions to extract the symmetric and unsymmetric vibration frequencies for a stress free cylinder. Table 4 compares the present three-dimensional elasticity solutions with those reported by Hutchinson (1981). The series type solutions, as mentioned by Hutchinson (1981), lead to upper bound values. The present method gives slightly lower frequency solutions, and is therefore considered to be more accurate. The percentage discrepancy between both methods is found to be well within 1.0% except for the SA-1 mode at $L/a = 10.0$ which gives a maximum discrepancy of approximately 1.3%. Thus it can be concluded that the solutions obtained using both approaches are in excellent agreement.

McMahon (1964) reported on the first experimental study on the free vibration of stress free cylindrical solids. A comprehensive set of vibration frequencies and mode shapes for cylinders of different sizes has been presented. Both aluminium and steel materials have been used in the fabrication of specimens. The present three-dimensional elasticity solutions are compared with the benchmark empirical data of McMahon (1964) for solid steel cylinders with length varying in the range of $0.5 \leq L/a \leq 2.50$. The frequency spectra of the first three lowest double symmetry (SS) vibration modes are presented in Fig. 3. McMahon (1964) devised a different characterisation of the vibration modes. The present double-symmetry modes fall into the set of results for circumferential order of zero and two in his experimental work. The symbols in Fig. 3 denote the experimental points reproduced from the frequency spectra of McMahon (1964). The Poisson ratio used for present computation is taken to be $\nu = 0.293$ (which corresponds to a steel material). The terms *odd* and *even* used in this figure describe antisymmetry and symmetry motions about the longitudinal direction.

From Fig. 3, it is evident that the present predictions are in excellent agreement with the experimental results. It is interesting to note that the odd longitudinal mode (denoted by triangles) passes gradually from SS-3 to SS-2 and merges with the fundamental double symmetry (SS-1) mode. Similar mode crossings of this nature are also observed for *odd* and *even* surface modes.

4. SOME REMARKS ON THE EXISTING SIMPLIFIED BEAM THEORIES

4.1 Preliminary remarks

From the present three-dimensional elasticity solutions some remarks on the existing simplified theories can be deduced. Models developed based on the simplified theories are

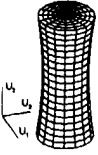

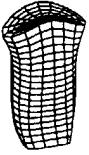
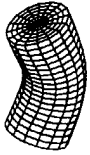





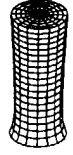
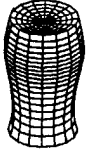
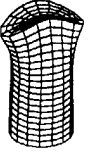
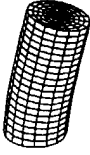





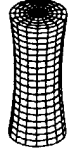
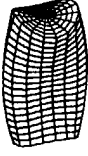
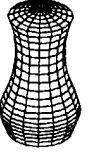
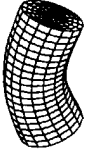





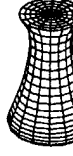

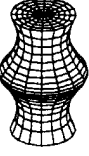
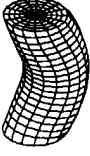





Boundary Conditions	Symmetry Classes and Mode Number								
	SS-1	SS-2	SS-3	SA-1	SA-2	SA-3	AA-1	AA-2	AA-3
<i>F-F</i>	 1.5467	 2.6265	 2.6612	 0.9594	 1.7751	 2.5937	 0.9742	 1.9483	 2.6265
<i>C-F</i>	 0.7934	 2.3055	 2.6443	 0.1976	 0.8061	 1.7152	 0.4871	 1.4612	 2.4354
<i>S-S</i>	 1.5467	 2.8703	 2.8856	 0.4965	 1.4278	 2.2838	 0.9742	 1.9483	 2.8703
<i>C-C</i>	 1.5942	 2.9551	 3.0261	 0.7752	 1.5469	 2.4745	 0.9742	 1.9483	 2.9225

Fig. 2. Three-dimensional deformed mode shapes of elastic circular cylinders with different boundary conditions ($L/a = 2.0$ and $\nu = 0.3$).

Table 4. Comparison of transverse vibration frequency parameters, $\lambda = \omega a \sqrt{\rho/E}$, for a stress free elastic circular cylinder with different length-to-diameter ratios

Mode	Source of results	Length-to-diameter ratio, L/a					
		1.0	1.25	2.0	2.50	5.0	10.0
SA-1	Hutchinson (1981)	2.47324	1.86902	0.95960	0.67752	0.20444	0.05524
	Present 3-D	2.47308	1.86876	0.95942	0.67736	0.20411	0.05453
		(-0.006)†	(-0.014)	(-0.019)	(-0.024)	(-0.162)	(-1.302)
SA-2	Hutchinson (1981)	2.66806	2.40800	1.77520	1.38064	0.49476	0.14476
	Present 3-D	2.66794	2.40782	1.77509	1.38048	0.49445	0.14407
		(-0.004)	(-0.007)	(-0.006)	(-0.009)	(-0.012)	(-0.479)
SA-3	Hutchinson (1981)	—	—	2.59376	2.10542	0.84590	0.26804
	Present 3-D	3.47491	2.68794	2.59371	2.10528	0.84559	0.26738
		—	—	(-0.002)	(-0.007)	(-0.037)	(-0.247)

† Figure in parenthesis denotes the discrepancy in %.

often used in engineering practice to provide approximate solutions. It is expedient to understand the underlying assumptions and inherent errors in these simplifications when using these models for analysis. Indiscriminate use of simplified models to tackle complex engineering problems may lead to undesirable results. The following section attempts to address some of the shortcomings in existing simplified theories by comparing with the present three-dimensional elasticity solutions.

4.2 One-dimensional wave equation

The one-dimensional wave equation for torsional and longitudinal modes has the following form

$$\frac{\partial^2 u}{\partial x^2} = \frac{1}{c^2} \frac{\partial^2 u}{\partial t^2} \tag{13}$$

where c is the wave velocity in the elastic media.

The general solution to eqn (13) for simple harmonic motion is written as

$$u(x, t) = \{C_1 \sin(\omega x/c) + C_2 \cos(\omega x/c)\} \sin \omega t. \tag{14}$$

The corresponding frequency equation for different end support conditions is derived from eqn (14) by substituting the appropriate boundary conditions.

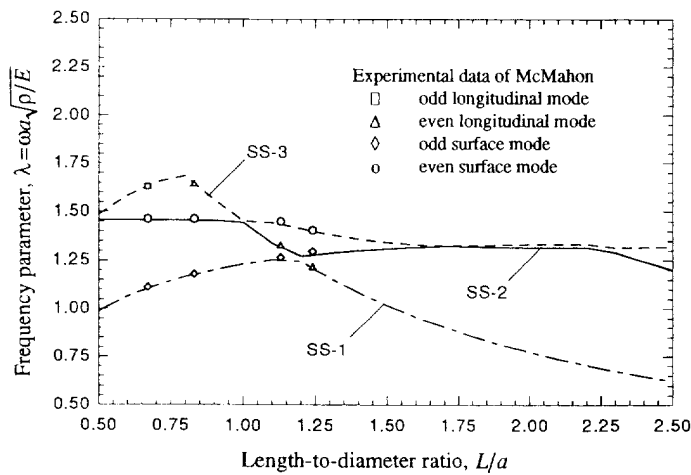


Fig. 3. Plot of first three lowest double-symmetry (SS) modes for a stress free elastic solid circular cylinder at different lengths ($\nu = 0.294$).

Table 5. Torsional vibration frequency parameter, $\lambda = \omega a \sqrt{\rho/E}$, from the three-dimensional linear elasticity method and the one-dimensional wave equation

Boundary condition	Mode	Source of results	Diameter-to-length ratio, a/L				
			0.1	0.2	0.3	0.4	0.5
<i>F-F</i> (<i>C-C</i>)	AA-1	1-D wave equation [†]	0.1948	0.3897	0.5845	0.7793	0.9742
		Present 3-D results	0.1948	0.3897	0.5845	0.7793	0.9742
	AA-2	1-D wave equation	0.3897	0.7793	1.1690	1.5587	1.9483
		Present 3-D results	0.3897	0.7793	1.1690	1.5587	1.9483
	AA-3	1-D wave equation	0.5845	1.1690	1.7535	2.3380	2.6265
		Present 3-D results	0.5845	1.1690	1.7535	2.3380	2.9225
<i>C-F</i>	AA-1	1-D wave equation [‡]	0.0974	0.1948	0.2922	0.3897	0.4871
		Present 3-D results	0.0974	0.1948	0.2922	0.3897	0.4871
	AA-2	1-D wave equation	0.2922	0.5845	0.8767	1.1690	1.4612
		Present 3-D results	0.2922	0.5845	0.8767	1.1690	1.4612
	AA-3	1-D wave equation	0.4871	0.9742	1.4612	1.9483	2.4354
		Present 3-D results	0.4871	0.9742	1.4612	1.9483	2.4354

Notes:

[†] For *F-F* and *C-C* elastic circular columns, the one-dimensional wave equation gives $\lambda = i\pi(a/L)\{2(1+\nu)\}^{-1/2}$; $i = 1, 2, 3, \dots$

[‡] For *C-F* elastic circular columns, the frequency solutions are $\lambda = i(\pi/2)(a/L)\{2(1+\nu)\}^{-1/2}$; $i = 1, 3, 5, \dots$

For torsional vibration, the parameter c is defined to be the shear wave velocity, $\sqrt{G/\rho}$, and the displacement variable, u , denotes the angular rotation. Table 5 presents the torsional frequency parameters for cylinders with *F-F*, *C-F* and *C-C* end support conditions. Solutions to the one-dimensional wave equations are deduced from Harker (1983). Not surprisingly, the torsional frequency predicted in both the one-dimensional wave equation and the three-dimensional linear elasticity solutions shows complete agreement for circular cylinders of different lengths.

When approximating the longitudinal vibration modes, the parameter c in eqn (13) becomes the stress wave velocity, $\sqrt{E/\rho}$. The one-dimensional wave equation for longitudinal vibration assumes negligible influence of lateral displacement upon the longitudinal vibration motions. For relatively short cylinders, however, the influence of lateral displacement can be significant. A correction to the one-dimensional wave equation for longitudinal motions has been suggested by Love (1927). The modified one-dimensional wave equation in the present notation, has the following form:

$$\frac{\partial^2 u}{\partial x^2} = \frac{1}{c^2} \left(\frac{\partial^2 u}{\partial t^2} - \nu^2 a^2 \frac{\partial^4 u}{\partial x^2 \partial t^2} \right). \tag{15}$$

The modified one-dimensional wave equation takes account of the inertia of the lateral motion indicated by the underlined term in eqn (15). For a *F-F* circular cylinder of finite length, L , the correction to the period of vibration was found by Lord Rayleigh (1945) to be in the ratio of:

$$1 : 1 + \left(\frac{n\nu\pi a}{4L} \right)^2. \tag{16}$$

In Table 6, a comparative study between the longitudinal vibration frequency parameter of circular cylinders computed from the one-dimension wave equation and the present three-dimensional elasticity solution is carried out. It is noted that longitudinal vibration frequencies obtained from the one-dimensional wave equation deviate significantly from the three-dimensional linear elasticity solutions as the diameter-to-length ratio increases beyond the range of $a/L \geq 0.3$. However, with the correction factor in eqn (16), the frequency parameters from the modified one-dimensional wave equation are found to correlate very well with the present three-dimensional elasticity solution for a circular cylinder with $a/L \leq 0.3$.

4.3. Timoshenko's shear deformable beam theory

The governing differential equations for transverse vibration of a prismatic elastic cylinder including the effects of shear deformation and rotary inertia are given by Young (1962) as:

$$\varphi'' + \frac{\kappa GA}{EI} (u' - \varphi) - \frac{\rho}{E} \ddot{\psi} = 0 \quad (17a)$$

$$\frac{\kappa G}{E} (\varphi' - u'') + \rho \ddot{u} = 0 \quad (17b)$$

where κ is the shear correction factor accounting for non-uniform shear stress distribution over the cross sectional area; E , G and A are the Young's modulus, shear modulus and cross sectional area of the cylinder, respectively. The displacement variable, u , represents transverse deflection and φ the corresponding slope during deflection.

The general solution to eqns (17a, b) can be derived from the theory of linear differential equation for simple harmonic vibration as:

$$u(x, t) = (C_1 \sin \alpha x + C_2 \cos \alpha x + C_3 \sinh \beta x + C_4 \cosh \beta x) \sin \omega t \quad (18a)$$

and

$$\varphi(x, t) = \left[\frac{(\kappa G/E)\bar{p}^2 + \alpha^2}{\alpha L} (C_1 \sinh \alpha x + C_2 \cosh \alpha x) + \frac{(\kappa G/E)\bar{p}^2 - \beta^2}{\beta L} (C_3 \sin \beta x - C_4 \cos \beta x) \right] \sin \omega t \quad (18b)$$

where

$$\alpha^2 = \frac{\bar{p}^2}{2} \left\{ \left[\left(1 - \frac{E}{\kappa G} \right)^2 + \frac{64}{\bar{p}^2} \left(\frac{L}{a} \right)^2 \right]^{1/2} - \left(1 + \frac{E}{\kappa G} \right) \right\} \quad (19a)$$

$$\beta^2 = \frac{\bar{p}^2}{2} \left\{ \left[\left(1 - \frac{E}{\kappa G} \right)^2 + \frac{64}{\bar{p}^2} \left(\frac{L}{a} \right)^2 \right]^{1/2} + \left(1 + \frac{E}{\kappa G} \right) \right\} \quad (19b)$$

and

$$\bar{p} = \omega L \sqrt{E_i \rho}. \quad (20)$$

Depending on the boundary conditions at both ends, the frequency equation derived from Timoshenko's beam theory has the form presented in Table 7. For a detailed derivation, readers are referred to Young (1962). The transcendental frequency equations are solved iteratively for the parameter, \bar{p} . In this study, the shear correction factor, κ , is taken to be 0.925 which is consistent with the value proposed by Timoshenko for a circular cross sectional beam.

Figures 4 and 5 depict the variation of transverse vibration frequency with respect to diameter-to-length ratio under different boundary conditions. The transverse vibrations of a F - F cylinder have been thoroughly treated by Hutchinson (1981). To be consistent with the notation introduced by Hutchinson (1981), the frequencies, $\bar{\lambda}$, for plotting purposes, have been redefined as

$$\bar{\lambda} = (L/a) \sqrt{\lambda}. \quad (21)$$

Some remarks are made from these plots. Firstly, it is observed that the predictions by Timoshenko's beam theory agree quite well with the present three-dimensional elasticity

Table 6. Comparison of longitudinal vibration frequency parameters, $\lambda = \omega a \sqrt{\rho/E}$, from the three-dimensional linear elasticity method and the one-dimensional wave equation

Boundary condition	Mode	Diameter-to-length ratio, a/L				
		0.1	0.2	0.3	0.4	0.5
<i>F-F</i>	SS-1	0.3140	0.6269	0.9376	1.2447	1.5467
		{0.3142}†	{0.6283}	{0.9425}	{1.2566}	{1.5708}
	SS-2	{0.3140}‡	[0.6269]	[0.9378]	[1.2455]	[1.5493]
		0.6269	1.2447	1.8414	2.3979	2.6265
		{0.6283}	{1.2566}	{1.8850}	{2.5133}	{3.1416}
		[0.6269]	[1.2455]	[1.8481]	[2.4271]	[2.9764]
SS-3	0.9378	1.8418	2.6426	2.6301	2.6612	
	{0.9425}	{1.8850}	{2.8274}	{3.7699}	{4.7124}	
	[0.9378]	[1.8481]	[2.7057]	[3.4908]	[4.1891]	
<i>C-F</i>	SS-1	0.1576	0.3158	0.4746	0.6339	0.7934
		{0.1571}	{0.3142}	{0.4712}	{0.6283}	{0.7854}
	SS-2	0.4724	0.9433	1.4094	1.8658	2.3055
		{0.4712}	{0.9425}	{1.4137}	{1.8850}	{2.3562}
	SS-3	0.7855	1.5570	2.2894	2.6434	2.6443
		{0.7854}	{1.5708}	{2.3562}	{3.1416}	{3.9270}
<i>C-C</i>	SS-1	0.3161	0.6342	0.9539	1.2743	1.5942
		{0.3142}	{0.6283}	{0.9425}	{1.2566}	{1.5708}
	SS-2	0.6312	1.2602	1.8786	2.4738	2.9551
		{0.6283}	{1.2566}	{1.8850}	{2.5133}	{3.1416}
	SS-3	0.9441	1.8669	2.7210	2.9188	3.0261
		{0.9425}	{1.8850}	{2.8274}	{3.7699}	{4.7124}

† Value in { } parenthesis denotes longitudinal vibration frequency computed from the one-dimensional wave equation.
 ‡ Value in [] parenthesis denotes frequency parameters computed from the modified one-dimensional wave equation.

Table 7. Boundary conditions and frequency equations of Timoshenko beam theory.

Type	Boundary conditions	Frequency equations
<i>F-F</i>	Symmetric modes $u'(0) - \varphi(0) = 0, \varphi(0) = 0$ $\varphi'(L/2) = 0, u'(L/2) - \varphi(L/2) = 0$	$\tan \frac{\beta}{2} + \frac{\beta}{\alpha} \frac{\alpha^2 + \bar{p}^2}{\beta^2 - \bar{p}^2} \tanh \frac{\alpha}{2} = 0$
	Antisymmetric modes $u(0) = 0, \varphi'(0) = 0$ $\varphi'(L/2) = 0, u'(L/2) - \varphi(L/2) = 0$	$\tan \frac{\beta}{2} - \frac{\beta}{\alpha} \frac{\alpha^2 - \bar{p}^2}{\beta^2 + \bar{p}^2} \tanh \frac{\alpha}{2} = 0$
<i>C-F</i>	$u(0) = 0, \varphi(0) = 0$ $u(L) - \varphi(L) = 0, \varphi'(L) = 0$	$2 + \frac{\alpha^2 - \beta^2}{\alpha\beta} \sinh \alpha \sin \beta$ $-\left(\frac{\beta^2 - \bar{p}^2}{\alpha^2 + \bar{p}^2} + \frac{\alpha^2 + \bar{p}^2}{\beta^2 - \bar{p}^2} \right) \cosh \alpha \cos \beta = 0$
<i>C-C</i>	Symmetric modes $u'(0) - \varphi(0) = 0, \varphi(0) = 0$ $u(L/2) = 0, \varphi(L/2) = 0$	$\tan \frac{\beta}{2} + \frac{\beta}{\alpha} \frac{\alpha^2 + \bar{p}^2 (\kappa G/E)}{\beta^2 - \bar{p}^2 (\kappa G/E)} \tan \frac{\alpha}{2} = 0$
	Antisymmetric modes $u(0) = 0, \varphi'(0) = 0$ $u(L/2) = 0, \varphi(L/2) = 0$	$\tan \frac{\beta}{2} - \frac{\beta}{\alpha} \frac{\alpha^2 - \bar{p}^2 (\kappa G/E)}{\beta^2 + \bar{p}^2 (\kappa G/E)} \tan \frac{\alpha}{2} = 0$

solutions for *F-F* cylinders up to ratio $a/L = 0.5$. Generally, closer correlation is found in the lower modes. Secondly, it is noted that for *C-F* and *C-C* cylinders, the discrepancies become significant especially at higher modes of vibration. It is concluded that the boundary conditions of cylinders may play an important role in the accuracy of refined beam theory.

5. PARAMETRIC INVESTIGATION

The plots of frequency parameters, $\bar{\lambda}$, versus length-to-diameter ratios are presented in Figs 6(a,b) and 7(a,b) for *F-F*, *C-F*, *S-S* and *C-C* end support conditions. The first

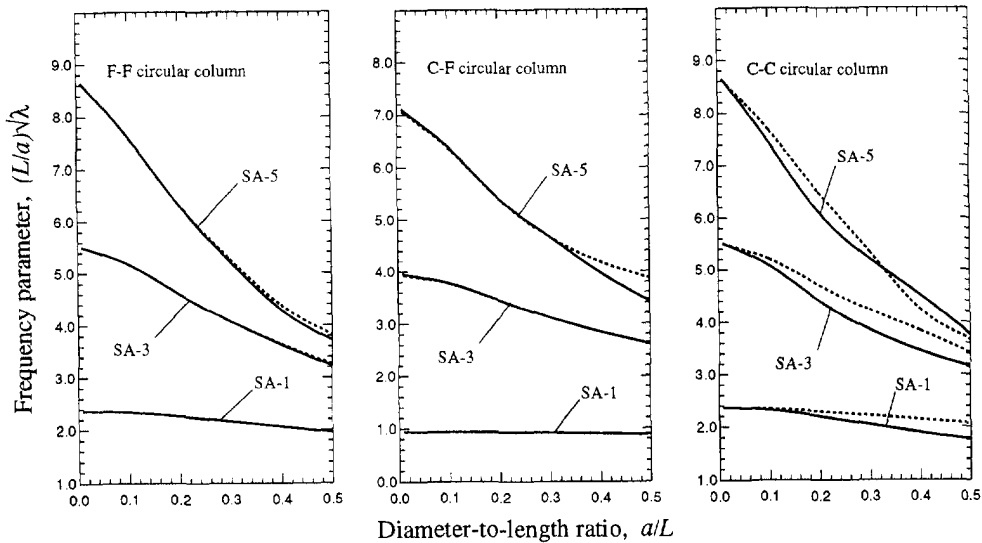


Fig. 4. Comparison of frequency parameters (modes 1, 3 and 5), $\bar{\lambda} = (L/a)\sqrt{\lambda}$, computed from the Timoshenko beam theory and the three-dimensional solutions for (a) a *F-F* circular cylinder, (b) a *C-F* circular cylinder, and (c) a *C-C* circular cylinder.

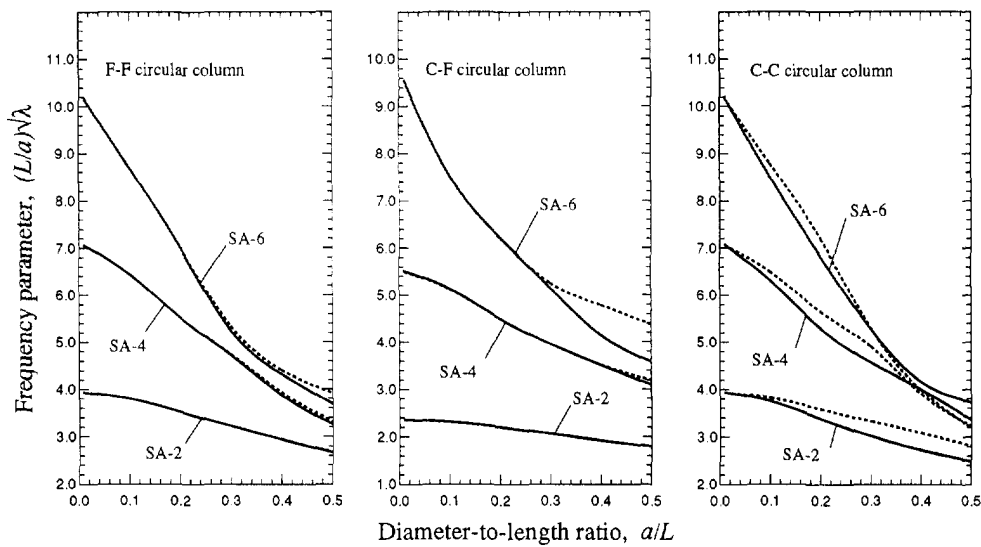


Fig. 5. Comparison of frequency parameters (modes 2, 4 and 6), $\bar{\lambda} = (L/a)\sqrt{\lambda}$, computed from the Timoshenko beam theory and the three-dimensional solutions for (a) a *F-F* circular cylinder, (b) a *C-F* circular cylinder, and (c) a *C-C* circular cylinder.

two frequencies, in the plots, corresponding to each symmetry class are presented. The symmetric-antisymmetric (SA) modes for circular cylinders are identical to the anti-symmetric-symmetric (AS) modes of vibration. Considering the effect of length-to-diameter ratio on the vibration frequency, it is observed that the frequency parameters increase monotonically as the length-to-diameter ratio increases. The variation is most significant for the SS and AA modes of vibration. However, the frequency variation with respect to the ratio L/a , for the SA and AS modes (which correspond to transverse bending motion about the x_1 and x_2 axes) is more gradual and tends to converge asymptotically to the Bernoulli-Euler beam solutions.

Considering the frequency plots for cylinders with stress free ends as shown in Fig. 6(a), it is observed that the fundamental vibration frequency at $L/a \leq 3.0$ is dominated by the first axial torsional mode (AA-1). At a higher length-to-diameter ratio, the transverse bending mode (SA-1) begins to dominate in the lower vibration spectrum and frequency

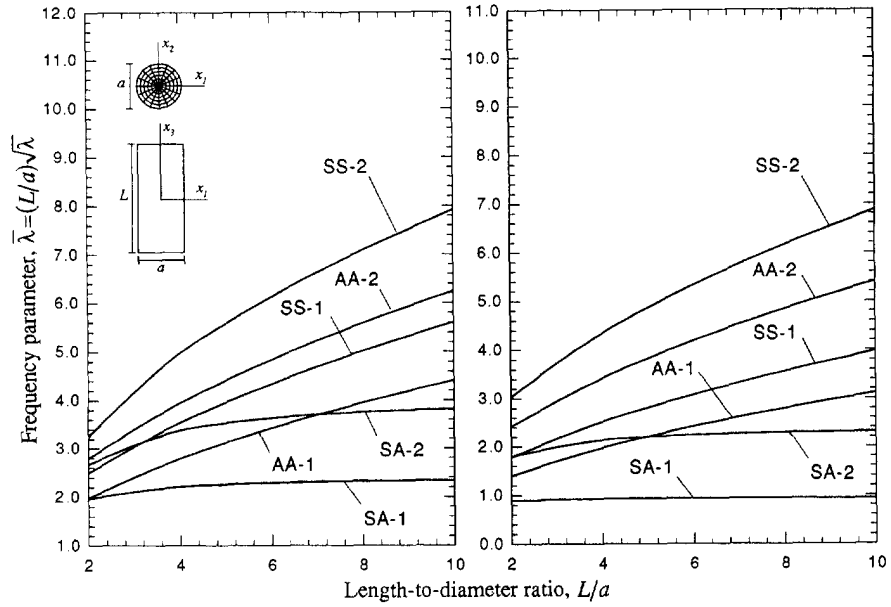


Fig. 6. Plots of frequency parameters $\bar{\lambda} = (L/a)\sqrt{\lambda}$ versus length-to-diameter ratio, L/a , for (a) a stress free elastic circular cylinder, and (b) a cantilevered elastic circular cylinder.

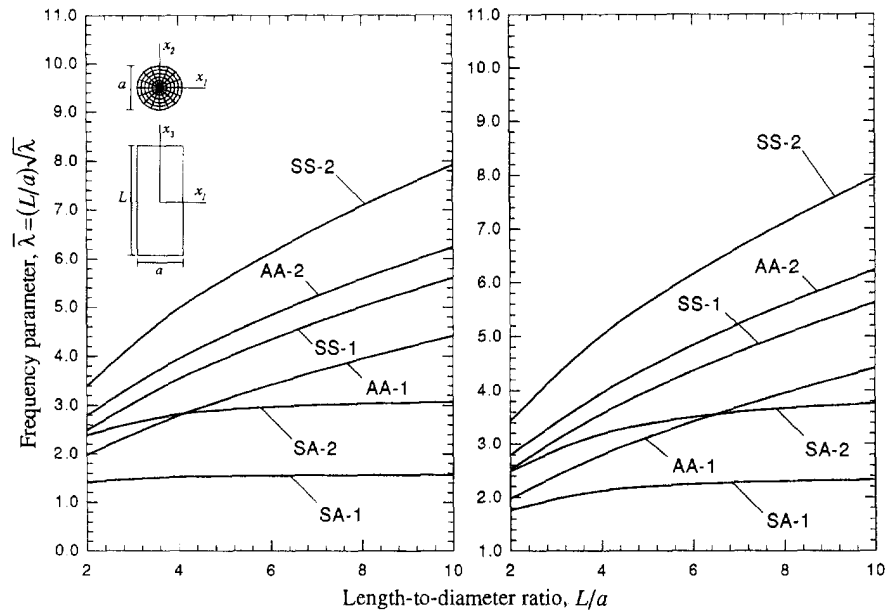


Fig. 7. Plots of frequency parameters $\bar{\lambda} = (L/a)\sqrt{\lambda}$ versus length-to-diameter ratio, L/a , for (a) a simply supported elastic circular cylinder, and (b) a fully clamped elastic circular cylinder.

crossing between AA-1 and SA-1 occurs. Depending on the end support conditions, further frequency crossing of this nature occurs at the higher modes. It is deduced that irrespective of the end support conditions, axial extensional (SS modes) motions always occur at much higher frequency of vibration.

6. CONCLUSIONS

A linear three-dimensional frequency equation for free vibration of circular cylinders has been reported. The method is relatively easy to implement and the results obtained are

found to be accurate when compared with the existing three-dimensional analytical solutions and experimental data.

Numerical convergence of frequency solutions is established as higher order polynomials are used in the computation. The convergence is found to be rapid and the use of symmetry consideration has greatly reduced the determinant size of the eigenvalue equation and further enhanced the computational efficiency of the method. Extensive frequency results and mode shapes are presented for cylinders with different combinations of end support conditions. From the current three-dimensional linear elasticity solutions, some remarks on existing one-dimensional wave equations for longitudinal and torsional vibration have been made. Particular attention is drawn to the Timoshenko shear deformable beam equation. The frequency solutions obtained from the refined theory are found to be acceptable for a F - F cylinder with diameter-to-length ratios of up to 0.5. For cylinders with C - F or C - C boundary conditions, the solution becomes inaccurate for higher modes and at higher diameter-to-length ratios.

REFERENCES

- Armenakas, A. E., Gazis, D. C. and Hermann, G. (1969). *Free Vibrations of Circular Cylindrical Shells*. Pergamon Press, Oxford.
- Cowper, G. R. (1966). The shear coefficient in Timoshenko's beam theory. *ASME J. Appl. Mech.* **33**, 335–340.
- Gladwell, G. M. L. and Tahbaldar, U. C. (1972). Finite element analysis of the axisymmetric vibrations of cylinders. *J. Sound Vibr.* **22**, 143–157.
- Gladwell, G. M. L. and Vijay, D. K. (1975). Natural frequencies of free finite-length circular cylinders. *J. Sound Vibr.* **42**, 387–397.
- Harker, R. J. (1983). *Generalized Methods of Vibration Analysis*. John Wiley, New York.
- Heyliger, P. R. and Jilani, A. (1992). The free vibrations of inhomogeneous elastic cylinders and spheres. *Int. J. Solids Structures* **22**, 2689–2708.
- Hutchinson, J. R. (1980). Vibrations of solid cylinders. *ASME J. Appl. Mech.* **47**, 901–907.
- Hutchinson, J. R. (1981). Transverse vibrations of beams, exact versus approximate solutions. *ASME J. Appl. Mech.* **48**, 923–928.
- Liew, K. M., Hung, K. C. and Lim, M. K. (1993). A continuum three-dimensional vibration analysis of thick rectangular plates. *Int. J. Solids Structures* **30**, 3357–3379.
- Liew, K. M., Hung, K. C. and Lim, M. K. (1994). Three-dimensional elasticity solutions to vibration of cantilevered skewed trapezoids. *AIAA J.* **32**, 2080–2089.
- Love, A. E. H. (1927). *A Treatise on the Mathematical Theory of Elasticity*. 4th ed. Cambridge University Press, Cambridge.
- McMahon, G. W. (1964). Experimental study of the vibrations of solid, isotropic elastic cylinders. *J. Acoust. Soc. Am.* **36**, 85–92.
- McMahon, G. W. (1970). Finite different analysis of the vibrations of solid cylinders. *J. Acoust. Soc. Am.*, **48**, 307–312.
- Rayleigh, J. W. S. (1945). *The Theory of Sound*. Vol. 1. Dover Publications, New York.
- Spence, G. B. and Seldin, E. J. (1970). Sonic resonances of a bar and compound torsion oscillator. *J. Appl. Phys.* **41**, 3383–3389.
- Stephen, N. G. (1978). On the variation of Timoshenko's shear coefficient with frequency. *ASME J. Appl. Mech.* **45**, 695–697.
- Timoshenko, S. P. (1921). On the correction for shear of the differential equation for transverse vibrations of prismatic bars. *Phil. Mag.* **41**, 744–746.
- Timoshenko, S. P. (1922). On the transverse vibrations of bars of uniform cross-section. *Phil. Mag.* **43**, 125–131.
- Timoshenko, S. P., Young, D. H. and Weaver, Jr., W. (1974). *Vibration Problems in Engineering*, 4th Edition. John Wiley, New York.
- Visscher, W., Migliori, A., Bell, T. M. and Reinert, R. A. (1991). On the normal modes of free vibration of inhomogeneous and anisotropic elastic objects. *J. Acoust. Soc. Am.* **90**, 2154–2162.
- Young, D. (1962). In *Continuous System, Handbook of Engineering Mechanics*, (Edited by W. Flügge). McGraw Hill, New York.